Journal of Anatomy

*J. Anat.* (2013) **223**, pp171–184 doi: 10.1111/joa.12071

# Chronotopographical distribution patterns of cell death and of lectin-positive macrophages/microglial cells during the visual system ontogeny of the small-spotted catshark *Scyliorhinus canicula*

Ruth Bejarano-Escobar,[1] Manuel Blasco,[2] Ana Carmen Durán,[3] Gervasio Martín-Partido[1] and Javier Francisco-Morcillo[1]

[1]*Departamento de Biología Celular, Facultad de Ciencias, Universidad de Extremadura, Badajoz, Spain*
[2]*Entomonuba S.L., Sevilla, Spain*
[3]*Departamento de Biología Animal, Facultad de Ciencias, Universidad de Málaga, Málaga, Spain*

## Abstract

The patterns of distribution of TUNEL-positive bodies and of lectin-positive phagocytes were investigated in the developing visual system of the small-spotted catshark *Scyliorhinus canicula*, from the optic vesicle stage to adulthood. During early stages of development, TUNEL-staining was mainly found in the protruding dorsal part of the optic cup and in the presumptive optic chiasm. Furthermore, TUNEL-positive bodies were also detected during detachment of the embryonic lens. Coinciding with the developmental period during which ganglion cells began to differentiate, an area of programmed cell death occurred in the distal optic stalk and in the retinal pigment epithelium that surrounds the optic nerve head. The topographical distribution of TUNEL-positive bodies in the differentiating retina recapitulated the sequence of maturation of the various layers and cell types following a vitreal-to-scleral gradient. Lectin-positive cells apparently entered the retina by the optic nerve head when the retinal layering was almost complete. As development proceeded, these labelled cells migrated parallel to the axon fascicles of the optic fiber layer and then reached more external layers by radial migration. In the mature retina, lectin-positive cells were confined to the optic fiber layer, ganglion cell layer and inner plexiform layer. No evident correlation was found between the chronotopographical pattern of distribution of TUNEL-positive bodies and the pattern of distribution of lectin-labelled macrophages/microglial cells during the shark's visual system ontogeny.

**Key words:** cell death; development; elasmobranch; macrophages; microglia; TUNEL technique; visual system.

## Introduction

Programmed cell death is an important mechanism involved in morphogenesis and histogenesis of the central nervous system (for a review, see Oppenheim, 1991). In the visual system several phases of cell death have been reported to occur during ontogeny (for a review, see Valenciano et al. 2009). First, morphogenetic cell death occurs during the optic vesicle and optic cup stages. It has been suggested that this programmed cell death is involved in sculpting the retina and facilitating the exit of optic fibres (García-Porrero et al. 1984; Cuadros & Ríos, 1988; Knabe & Kuhn, 1998; Laemle et al. 1999; Trousse et al. 2001; Candal et al. 2005; Rodríguez-Gallardo et al. 2005). The early neural cell death then affects retinal ganglion cells during the period of differentiation (Cuadros & Ríos, 1988; Martín-Partido et al. 1988; Pequignot et al. 2003; Candal et al. 2005). Finally, neurotrophic cell death is regulated through the competition of limited amount of neurotrophins released by the target cells (Young, 1984; Cook et al. 1998; Marín-Teva et al. 1999; Mayordomo et al. 2003; Pequignot et al. 2003; Francisco-Morcillo et al. 2004; Candal et al. 2005). This phase is critical for the establishment of a definitive pattern of neuronal connections. Concomitant with these areas of cell death during retinal differentiation, dying cells have also been described in the optic pathways (Horsburgh & Sefton, 1986; Navascués et al. 1988; Moujahid et al. 1996; Rodríguez-Gallardo et al. 2005; Hidalgo-Sánchez et al. 2007; Bejarano-Escobar et al. 2011). These authors identified dead cells in the ventral wall of the optic stalk which is

*Correspondence*
*Javier Francisco-Morcillo, Departamento de Biología Celular, Facultad de Ciencias, Universidad de Extremadura, Avda. de Elvas s/n, 06006 Badajoz, Spain. T/F: + 34 92 4289411; E: morcillo@unex.es*

Accepted for publication *16 May 2013*
Article published online *13 June 2013*

subsequently occupied by optic axon fascicles. Therefore, cell death in the developing optic nerve precedes axon growth both spatially and temporally.

Cell debris released during ontogeny is mostly removed by heterophagy. Thus, during the initial phases of nervous system development, the cell fragments are phagocytosed by neuroepithelial cells resembling those destined to degenerate, as has previously been described in our laboratory (Navascués et al. 1988; Martín-Partido & Navascués, 1990; Bejarano-Escobar et al. 2011). Furthermore, in the differentiating vertebrate retina Müller cells appear able to phagocytose cell debris (Egensperger et al. 1996; Marín-Teva et al. 1999; Francisco-Morcillo et al. 2004). However, cell debris released in the retinal tissue during the cell death process is also removed by macrophages and microglial cells during normal development (Hume et al. 1983; Marín-Teva et al. 1999; Knabe et al. 2000; Rodríguez-Gallardo et al. 2005; Santos et al. 2008; Bejarano-Escobar et al. 2011). Cell death has been proposed as the stimulus for the entry of microglial precursors into the central nervous system (Perry & Gordon, 1991; Thanos et al. 1996). Thus, macrophages and microglial precursors are in chronotopographical coincidence with cell death areas in the developing visual system (Hume et al. 1983; Schnitzer, 1989; Egensperger et al. 1996; Moujahid et al. 1996; Rodríguez-Gallardo et al. 2005; Santos et al. 2008; Bejarano-Escobar et al. 2011). Arguing against the hypothesis that cell death is the factor that attracts microglial precursors into the central nervous system are the facts that many of these precursors enter the retina of mammals well before the period of neuronal death (Ashwell, 1989; Díaz-Araya et al. 1995). Furthermore, in the avian developing retina, microglial cells traverse the inner nuclear layer (INL) only after cell death has ceased in that layer (Marín-Teva et al. 1999).

Most of the studies cited above were conducted on the developing retina of birds and mammals. There have only been a few specific studies of cell death during fish retinogenesis. Thus, in fast-developing fish species such as the African cichlid, *Haplochromis burtoni* (Hoke & Fernald, 1998), zebrafish (Cole & Ross, 2001), medaka (Iijima & Yokoyama, 2007) and Senegalese sole (Bejarano-Escobar et al. 2010), cell death during ontogeny of the retina is restricted to sparse cells, generally well separated, with no clear concentration or pattern. However, three well-defined periods of naturally occurring cell death have been reported during retinal ontogeny of slow-developing fish species (Candal et al. 2005).

Previous studies have shown that fish retinal microglia become activated in response to different injuries (Velasco et al. 1995; Jimeno et al. 1999, 2003; Bailey et al. 2010; Bejarano-Escobar et al. 2012b). Degenerating cells alert microglia, leading to activation, local proliferation, migration towards the injured tissue, and enhanced phagocytosis of cell debris. However, little information is available about microglial invasion in the developing fish visual system. The temporal and spatial patterns of retinal macrophage invasion and their phenotypic transition to early microglia in the developing zebrafish visual system has been described using the *in situ* hybridization technique for the *L-plastin* gene (Herbomel et al. 2001).

Recently, detailed studies of the major events during retinogenesis of the small-spotted catshark, *Scyliorhinus canicula* (Linnaeus, 1758) have been performed (Ferreiro-Galve et al. 2008, 2010a,b, 2012; Bejarano-Escobar et al. 2012a). We consider that this cartilaginous fish species may be particularly suitable for descriptions of ontogenetic processes because of its slow growth and large eyes. These features allow a detailed analysis of developmental processes, potentially yielding more details than the fast-developing species commonly used as fish models. We studied the spatiotemporal patterns of TUNEL-positive bodies and lectin-positive cells during development of the visual system in embryos, juveniles and adults of this shark species. To the best of our knowledge, this is the first study investigating the possible relationship between ontogenetic cell death and macrophage/microglial cells during development of the fish visual system.

## Materials and methods

### Experimental animals

Fertilized eggs were obtained from adult females collected in the western Mediterranean by local fishing vessels. The eggs were raised in fresh seawater tanks in standard conditions of 15–18 °C. At this temperature the average time of incubation was 175 days. The eggs were opened after we had made a rough estimate of the degree of developmental of the embryos through the transparent walls of the capsule, and the embryos were carefully removed. The embryonic stages of *S. canicula* were identified by their external features following Ballard et al. (1993). We divided the St32 into St32-early and St32-late (see Bejarano-Escobar et al. 2012a). The embryonic stages and the number (*n*) of processed animals analysed were: stage18 (St18; $n = 3$), St19 ($n = 4$), St20 ($n = 4$), St21 ($n = 4$), St22 ($n = 4$), St23 ($n = 4$), St24 ($n = 5$), St25 ($n = 4$), St26 ($n = 4$), St27 ($n = 4$), St28 ($n = 4$), St29 ($n = 4$), St30 ($n = 4$), St31 ($n = 5$), St32-early ($n = 4$), St32-late ($n = 3$), St33 ($n = 5$), St34 ($n = 5$). Furthermore, the retinas of 10 juveniles, ranging from hatching day (postnatal day 0; P0) to P7, and two adult specimens were also processed. Figure 1 shows embryos belonging to developmental stages ranging from St18 to St26. The rest of the shark embryological stages included in the present study have been presented previously by Bejarano-Escobar et al. (2012a).

### Tissue preparation

Adequate measures were adopted to minimize animal pain or discomfort. All procedures followed the guidelines issued by the Animal Care and Use Committee of the University of Extremadura. Embryos, newly hatched and adult specimens were overanaesthetized with 0.04% tricaine methane sulphonate (MS-222; Sigma Chemical Co., Poole, UK) in elasmobranch buffer (EB; 16.38 g $L^{-1}$ NaCl, 0.89 g $L^{-1}$ KCl, 1.11 g $L^{-1}$ $CaCl_2$, 0.38 g $L^{-1}$ $NaHCO_3$,

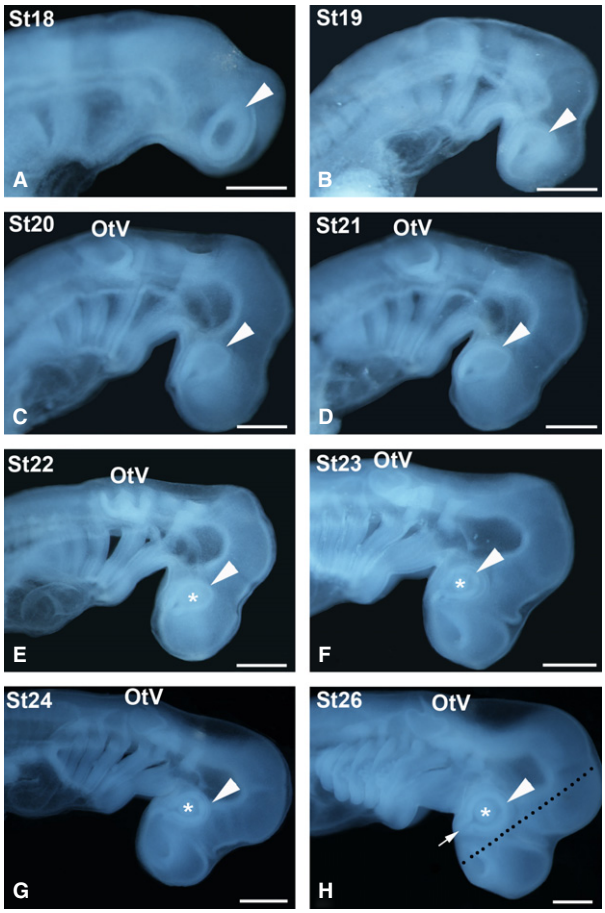


**Fig. 1** Stereomicroscope images of early embryos of small-spotted catshark used in the present study, according to the developmental stages (St) of Ballard et al. (1993). During the stages represented here (St18–24, 26) the metamerization of the pharynx and completion of the somite set occurs. The pharyngeal pouches become progressively visible from St18 to St20 (A-C). Pharyngeal clefts progressively open from St21 onwards (D-H). The optic anlage is clearly visible from St18 onwards (arrowheads), as well as the lens rudiment from St22 onwards (asterisks; E-H). The dotted line in (H) indicates the frontal plane of the section, parallel to the ventral optic fissure (arrow). OtV, otic vesicle. Scale bars: 1 mm.

0.06 g $L^{-1}$ $NaH_2PO_4$, 21.6 g $L^{-1}$ urea, pH 7.2) or seawater, respectively, and then fixed (see below). Chronotopographical distribution patterns of TUNEL-positive bodies and lectin-positive cells in the small-spotted catshark retina were examined in cryostat sections. Embryos and hatchlings were fixed by immersion in 4% paraformaldehyde (PFA) in EB (PFA 4%) or MAW (methanol/acetone/water 2 : 2 : 1), for 12–24 h depending on their size, at 4 °C. Adult sharks were previously perfused *in situ* with EB followed by 4% PFA, and post-fixed by immersion for 6 h at 4 °C in the same fixative. The eyes were removed and immersed for 12 h in the same fixative solution. Tissues were gradually hydrated and immersed in PBS, then cryoprotected in 15% sucrose solution in 0.1 M phosphate-buffered saline (PBS), soaked in embedding medium, frozen, and freeze-mounted onto aluminium sectioning blocks. Cryostat sections, 15 μm thick, were cut in frontal (parallel to the optic fissure, see Fig. 1H) or sagittal planes with respect to the brain. Consecutive sections were mounted as parallel sets on SuperFrost©Plus slides (Menzel-Glaser, Germany), and were treated alternately with the TUNEL technique or lectin histochemistry (see below).

### TUNEL technique

Because most cell death processes during development occur by apoptosis (Yeo & Gautier, 2003; Nagata, 2005), more recent approaches to map areas of cell death in the visual system are based on the detection of DNA fragmentation on cryosections using the TUNEL (terminal deoxynucleotidyl transferase-mediated deoxyuridinetriphosphate nick end-labelling) technique (Cook et al. 1998; Marín-Teva et al. 1999; Pequignot et al. 2003; Francisco-Morcillo et al. 2004; Bejarano-Escobar et al. 2010, 2011; *In situ* Cell Death Detection Kit, POD, from Roche Molecular Biochemicals, Mannheim, Germany). The TUNEL technique was performed as described in Bejarano-Escobar et al. (2010). In control sections in which the enzyme TdT was omitted from the reaction solution, no stained nuclei were observed.

### Lectin histochemistry

We have used B4 isolectin derived from *Griffonia simplicifolia* (GSL; Sigma, L3759) and the lectin obtained from *Lycopersicum esculentum* (tomato lectin, TL; Sigma, L0651). These lectins recognize macrophages and microglial cells in the nervous system of several vertebrates (Ashwell, 1990; Streit et al. 1990; Kaur & Ling, 1991; Acarín et al. 1994; Santos et al. 2008; Bejarano-Escobar et al. 2011), including fish (Velasco et al. 1995; Jimeno et al. 1999; Bejarano-Escobar et al. 2012b). Lectin histochemistry was performed as described in Bejarano-Escobar et al. (2011, 2012b). No signal was found in histochemical controls that were made omitting the lectin.

### Image acquisition and processing

Digital images of embryos and postnatal specimens were captured with a DS-5Mc Digital Camera (Nikon) attached to a Stereoscopic Microscope SMZ-1000 (Nikon). The sections were observed using an epifluorescence, bright field Nikon Eclipse 80i microscope, and photographed using an ultrahigh-definition Nikon digital camera DXM1200F. Figures were assembled and images were corrected for brightness and contrast in Adobe PHOTOSHOP (vCS4).

## Results

### Distribution of TUNEL-positive bodies in the deve -loping visual system of the small-spotted catshark

*Early development of the visual system (St18–St30)*

During the optic vesicle stage (St18–20) TUNEL-positive bodies were randomly scattered throughout the neuroepithelial wall of the optic vesicle (Fig. 2A,B). Coinciding with the onset of invagination and during optic cup stages (St21–23), abundant TUNEL-positive bodies were concentrated in two areas. The first was located in the dorsal part of the optic cup rim, both in the presumptive neural retina (pNR) and in the presumptive retinal pigment epithelium (pRPE; Figs 2C,D,F,G and 3A,C-E). The second area was observed in the presumptive optic chiasm (Figs 2C,E,F,H and

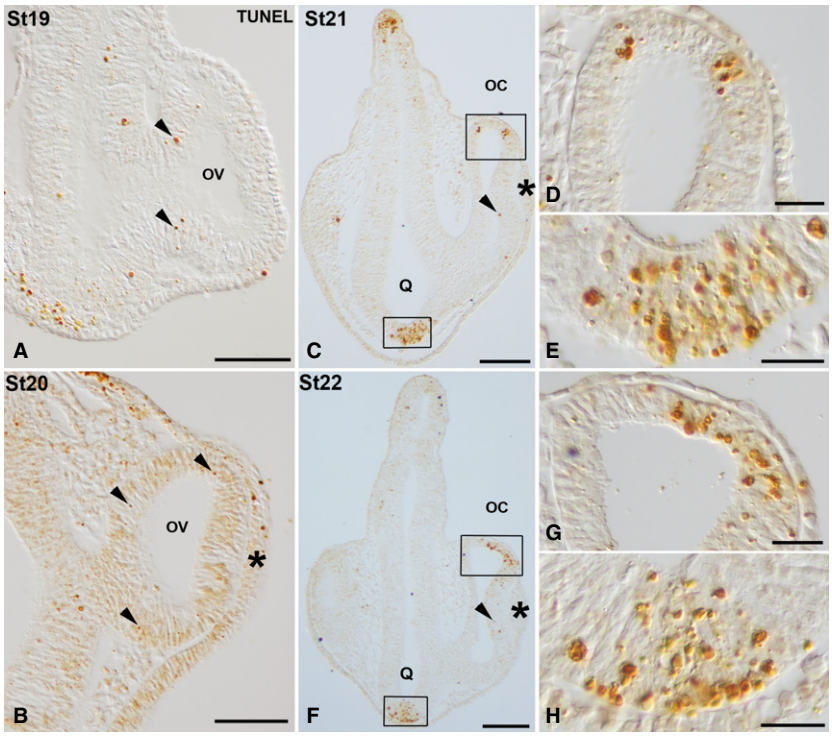


**Fig. 2** TUNEL-positive bodies in the developing visual system of small-spotted catshark embryos during St19 (A), St20 (B), St21 (C-E) and St22 (F-H). Frontal cryosections were treated according to the TUNEL method. Lens placode is indicated in panels (B,C,F) by asterisks. Boxed areas in (C) and (F) are shown at higher magnification in (D,E) and (G,H), respectively. In all panels, dorsal is up. During these early stages, sparse TUNEL-positive bodies were observed in the neuroepithelium of the optic anlage (arrowheads in A,B) and in the neuroepithelial cells of the presumptive neural retina (arrowheads in C,F). Areas with abundant TUNEL-positive bodies were detected by St21–22 in the dorsal-most part of the optic cup (C,D,F,G) and in the presumptive optic chiasm (C,E,F,H). oc, optic cup; ov, optic vesicle; Q, optic chiasm. Scale bars: 200 μm (A-C,F); 50 μm (D,E,G,H).

3A,B). TUNEL-staining was also detected in the anterior region of the lens rudiment throughout stages 23–25 (Figs 3A,C and 4A,B), and had almost disappeared by St26 (Fig. 4C). Moreover, between St23 and St24, TUNEL-positive bodies were dispersed throughout the neural retina (Figs 3A,F and 4A). However, between St25 and St29, TUNEL-positive bodies were absent from the neural retina (Fig. 4B–H). By St25 and St 26, TUNEL-positive pRPE cells adjacent to the distal optic stalk were detected (Fig. 4B,C). From St27 to St29, TUNEL-positive bodies were concentrated in the dorsal and ventral wall of the distal half of the optic stalk as well as in the pRPE that surrounded the optic nerve head (Fig. 4D-H).

*Differentiating retina (St31 to P0)*

We have recently shown that cell differentiation and histogenesis in the developing retina of the small-spotted catshark occurs following central-to-peripheral and vitreal-to-scleral gradients (Bejarano-Escobar et al. 2012a). The topographical patterns of distribution of TUNEL-positive bodies follow the same gradients, and are concomitant with the retinal layering. Thus, at St31, retinal lamination was restricted to the central retina, showing a ganglion cell layer (GCL) and an external neuroblastic layer (NbL; Fig. 5A). At this stage, TUNEL-positive bodies were sparse and dispersed throughout the central region of the neural retina, but mainly concentrated in the GCL (Fig. 5A). At stage 32-early, coinciding with the emergence of the OPL, although sparse TUNEL-positive bodies were observed in the GCL, most of them were located in the scleral half of the inner nuclear layer (INL; Fig. 5B). By St32-late and St33, TUNEL-positive bodies were absent from the GCL, but many of them were observed in the scleral half of the INL (Fig. 5C,D). Sparse TUNEL-positive photoreceptors were also found (Fig. 5C,D). Between St34 and the hatching stage (postnatal day 0, P0), TUNEL-positive bodies progressively disappeared from the INL and became restricted to the ONL (Fig. 5E,F). TUNEL signal was absent in P7 and in adult retinas (not shown). Therefore, the distribution of TUNEL-positive bodies during shark retinal histogenesis followed a vitreal-to-scleral gradient.

## Lectin-positive cells in the developing visual system of the small-spotted catshark

Abundant cells were histochemically labelled using the B4 isolectin derived from *Griffonia simplicifolia* (GSL) and the lectin obtained from *Lycopersicum esculentum* (tomato, TL). These lectins have been used to identify macrophages and microglial cells in the nervous system of various vertebrates (Ashwell, 1990; Streit et al. 1990; Kaur & Ling, 1991; Acarín et al. 1994; Knabe et al. 2000; Bejarano-Escobar et al. 2011), including fish (Velasco et al. 1995; Bejarano-Escobar et al. 2012b). Adjacent sections from the visual system of early embryos and hatchlings were treated according to the lectin histochemical technique (see Materials and methods). In the early embryonic specimens many large round cells located in the head mesenchyme were labelled with the two lectins (Fig. 6A,B). Furthermore, migrating amoeboid cells adhering to the retinal vitreal surface were labelled in the

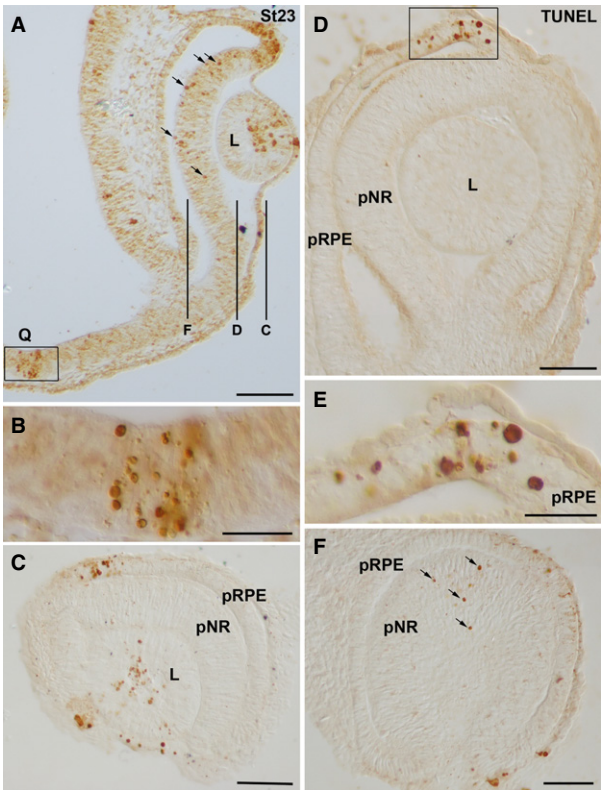


**Fig. 3** Spatial distribution of TUNEL-positive bodies in the developing visual system of small-spotted catshark embryos at St23. Frontal (A,B) and sagittal (C–F) cryosections were treated according to the TUNEL technique. (C,D,F) Overviews of sections at the level indicated in (A). Boxed areas in (A) and (D) are shown at higher magnification in (B) and (E), respectively. In all panels, dorsal is up. TUNEL-positive bodies were concentrated at the dorsal-most part of the optic cup (A,C-E), at the presumptive optic chiasm (A,B), and at the anterior region of the lens vesicle (A,C). Many TUNEL-positive bodies were dispersed throughout the undifferentiated neural retina (arrows in A,F). Notice that an undifferentiated spherical lens is present at this stage (A,C,D). L, lens; pNR, presumptive neural retina; pRPE, presumptive retinal pigment epithelium; Q, optic chiasm. Scale bars: 100 μm (A,C,D,F); 50 μm (B); 25 μm (E).

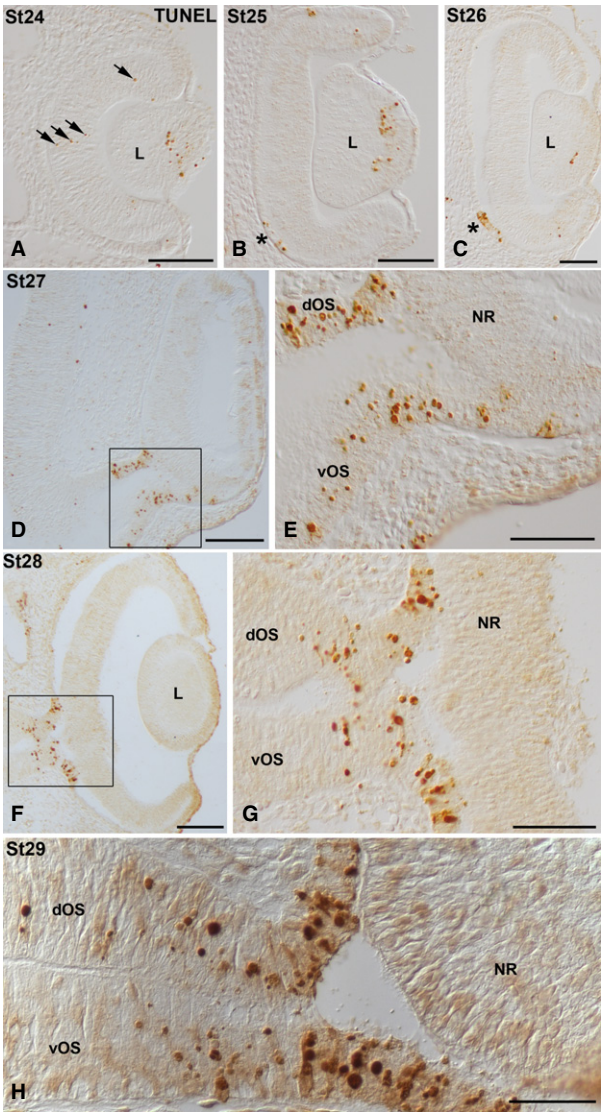


**Fig. 4** TUNEL-positive bodies in the developing visual system of small-spotted catshark embryos during St24 (A), St25 (B), St26 (C), St27 (D,E), St28 (F,G) and St29 (H). Frontal cryosections were treated according to the TUNEL method. In all panels, dorsal is up. Boxed areas in (D) and (F) are shown at higher magnification in (E) and (G), respectively. TUNEL-positive bodies were concentrated in the anterior region of the lens vesicle between St24 and St26 (A-C). Sparse TUNEL-positive bodies were dispersed throughout the undifferentiated neural retina (arrows in A) and restricted to the pRPE in the vicinity of the optic stalk (asterisks in B,C). Between St27 and St29, TUNEL labeling was detected in the dorsal and ventral regions of the distal half of the optic stalk, and in the presumptive retinal pigment epithelium that surrounds the optic nerve head (D-H). dOS, dorsal optic stalk; L, lens; NR, neural retina; pRPE, presumptive retinal pigment epithelium; vOS, ventral optic stalk. Scale bars: 100 μm (A-C); 200 μm (D,F); 50 μm (E,G); 30 μm (H).

vitreous cavity (Fig. 6A,B). Ramified cells distributed throughout the IPL were also identified with both lectins in the postnatal retina (Fig. 6C-F). Therefore, the same populations of cells were labelled with both lectins used. In the text, we will use 'lectin-positive cells' to refer to the cells labelled with either of the lectins.

Between St16 and St31, lectin-positive cells were absent from the developing retina and optic pathways. However, by these early stages (St20–28) many lectin-positive cells were observed in the adjacent mesenchymal tissue around the eye (not shown). At St29, labelled cells could be recognized in the vitreous body (Fig. 7A-C), some of them closely adhering to the lens (Fig. 7A,B). Other labelled cells were located in the lens/ectoderm interface (Fig. 7A,B). Although many lectin-positive cells were observed in the head mesenchyme (Fig. 7A,D), neither the neural retina nor the optic nerve presented lectin-positive cells (Fig. 7A, D). At St32-early, lectin-positive cells were distributed relatively uniformly along the optic nerve (Fig. 7E). Some of the labelled cells exhibited bipolar cell bodies oriented

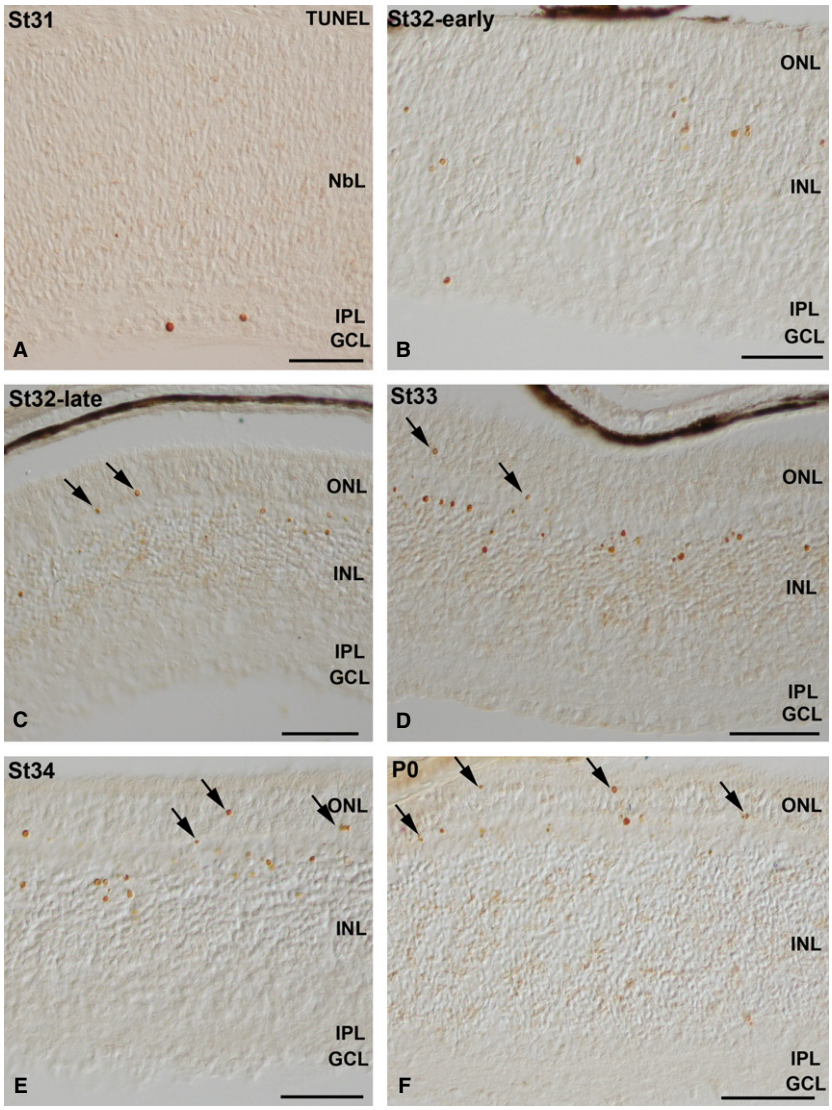


**Fig. 5** TUNEL-positive bodies in the differentiating central retina of small-spotted catshark embryos between embryonic St31 and St34 (A-E) and at the hatching stage (postnatal day 0, P0; F). Transverse retinal cryosections were treated according to the TUNEL technique. Sparse TUNEL-positive bodies were observed in the GCL at St31 (A). As development proceeded, TUNEL-positive bodies were mainly located in the external region of the INL (B-E) and in the ONL (arrows in C,D,F). GCL, ganglion cell layer; INL, inner nuclear layer; IPL, inner plexiform layer; NbL, neuroblastic layer; ONL, outer nuclear layer. Scale bars: 100 μm (A-D,G,H); 10 μm (E,F).

parallel with the optic nerve axons (Fig. 7F). There were also rounded (Fig. 7G) and elongated poorly ramified cells (Fig. 7H). At this stage, the first lectin-positive cells appeared in the neural retina in the immediate vicinity of the optic nerve head, located near the vitreal surface (Fig. 7E,I). At St32-late, abundant, more intensely stained lectin-positive cells were recognizable in sections to the distal (Fig. 7J) and proximal (Fig. 7K) optic nerve. These lectin-positive cells became more ramified, showing a more complex morphology (Fig. 7J,K). At St33 many lectin-positive ramified cells were found in the optic nerve (Fig. 8A-D) and in the vitreal-most part of the central neural retina (not shown). Amoeboid round lectin-labelled cells were also recognized in the peripheral retina near the vitreal surface (Fig. 8E,F). At St34, the IPL of the central and peripheral retina contained many amoeboid lectin-positive cells (Fig. 8G–J). Transverse optic nerve sections revealed that the lectin-positive cells were homogeneously distributed (Fig. 8K). At the hatching stage (P0), abundant lectin-positive cells with fine extended processes that coursed parallel to the optic axons could be observed in the optic nerve (Fig. 9A,B). In the central retina, labelled ramified cells continued to be observed, mainly in the IPL (Fig. 9a,c,f). In this layer, lectin-positive cells were arranged in a stratified manner. Thus, labelled cells were located in the border between the INL and the IPL, in the border of the IPL with the GCL, and in the middle of the IPL (Figs 9F and 6C–F). In the peripheral retina, round to slightly elongated labelled cells were found in the IPL and the optic fibre layer (OFL; Fig. 9D,E). At the adult age, ramified lectin-positive cells were mainly found in the IPL in the entire retina, with some radially oriented processes (Fig. 9G). Note that even at the adult ages, lectin-positive cells continued to be excluded from the more scleral layers, including the OPL (Fig. 9G). Lectin-positive cells in the adult optic nerve could also be observed (Fig. 9H).

Taken together, our findings indicate that lectin-positive cells were not in chronotopographical coincidence with

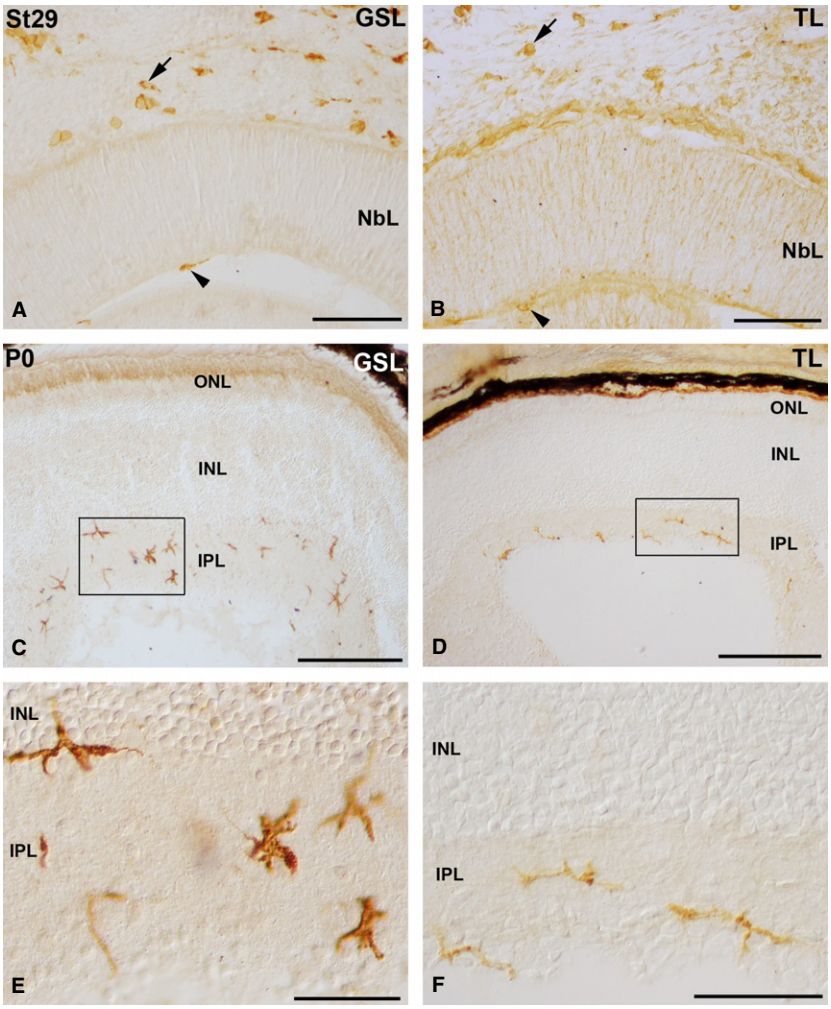


**Fig. 6** Lectin-positive cells in the retina of St29 embryos (A,B) and hatchlings (C-F) of small-spotted catshark. Cryosections were treated according to GSL (A,C,E) or TL (B,D,F) histochemistry technique. Boxed areas in (C) and (D) are shown at higher magnification in (E) and (F), respectively. Many round/amoeboid lectin-positive cells appeared in the mesenchyme (arrows in A,B) and in the vitreous cavity (arrowheads in A,B) during embryonic stages. Abundant ramified stellate lectin-positive cells were observed mainly in the IPL of the shark retina at the hatching stage (C-F). GSL, *Griffonia simplicifolia* lectin; INL, inner nuclear layer; IPL, inner plexiform layer; NbL, neuroblastic layer; ONL, outer nuclear layer; TL, tomato lectin. Scale bars: 100 μm (A,B); 200 μm (C,E) 50 μm (D,F).

regions with abundant TUNEL-positive bodies. Thus, the analysis of alternate consecutive sections treated with the TUNEL-technique or lectin histochemistry (see Materials and methods) showed no evident correlation between the chronotopographical pattern of distribution of TUNEL-positive bodies and lectin-positive cells during the development of the small-spotted catshark's visual system. The major findings obtained in this study are summarized in Fig. 10.

## Discussion

### Spatiotemporal distribution of cell death in the *S. canicula* developing visual system

A detailed distribution of dying cells during development of the visual system in the small-spotted catshark was observed using the TUNEL technique on cryosections. This technique allows the detection of DNA fragmentation characteristic of cell degeneration. Previous works in our laboratory have shown that this is an efficient method to detect dying cells in the developing visual system of several vertebrates, such as fish (Bejarano-Escobar et al. 2010), reptiles (Francisco-Morcillo et al. 2004) or mammals (Rodríguez-Gallardo et al. 2005; Bejarano-Escobar et al. 2011). The shape and size of TUNEL-positive bodies in the developing *S. canicula* visual system is similar to that observed in other vertebrates. Therefore, TUNEL technique constitutes a reliable method to map the regions of programmed cell death in the developing visual system of *S. canicula*.

*Cell death during morphogenesis of the optic vesicle and the optic cup*

The incidence of cell death in *S. canicula* embryos from the optic vesicle to pre-laminated retina stages (St18–St30) is discussed in this section. Our findings are consistent with several reports on very young mammalian and avian embryos, which show that dying cells are clustered in both space and time (for a review, see Valenciano et al. 2009). Thus, there were four areas of cell degeneration observed during early shark visual system development. (i) An area of cell degeneration in the dorsal part of the optic cup is present through St21–St23, as has previously been described in the chick (García-Porrero et al. 1984; Trousse et al. 2001) and the tree shrew *Tupaia belangeri* (Knabe et al. 2000).

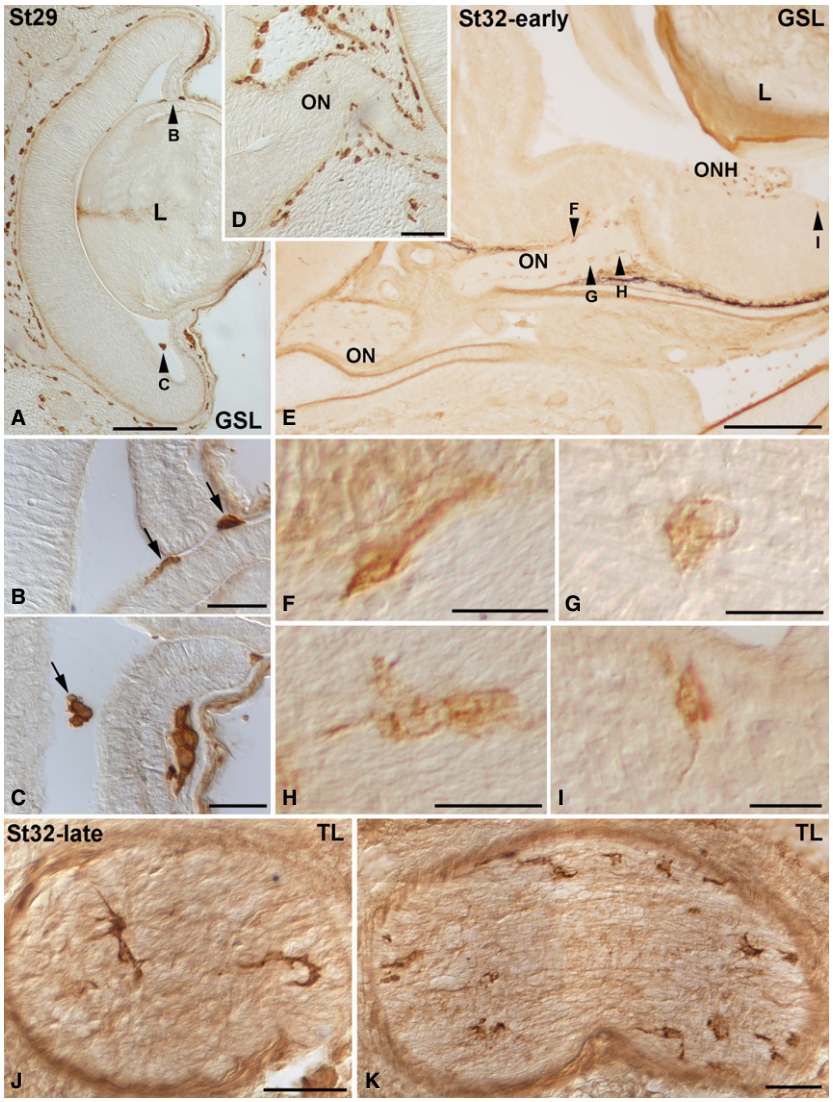


**Fig. 7** Lectin-positive cells in the developing visual system of small-spotted catshark embryos at St29 (A-D), St32-early (E-I) and St32-late (J,K). Frontal (A-I) and sagittal (J,K) cryosections of the head were treated according to the GSL (A-I) and TL (J,K) histochemistry technique. Arrowheads in (A) and (E) point to cells shown at higher magnification in (B,C,F-I). In all panels, dorsal is up. At St29, GSL histochemistry allows the visualization of sparse labelled cells in the vitreous cavity (A, arrows in B,C), some of them attached to the epithelial wall of the lens vesicle (arrows in B). Note that by this stage the optic nerve was devoid of labelled cells (D). GSL-positive cells were uniformly distributed along the length of the optic nerve at St32-early (E). These cells were bipolar (F), ovoid (G) and elongate and poorly ramified (H). A few lectin-positive cells were at first observable close to the vitreal surface of the retina in regions adjacent to the ONH (E,I). In the St32-late optic nerve, TL-positive cells had a more complex morphology. GSL, *Griffonia simplicifolia* lectin; L, lens; ON, optic nerve. ONH, optic nerve head; TL, tomato lectin. Scale bars: 200 μm (A); 50 μm (B,C,J, K); 100 μm (D); 500 μm (E); 20 μm (F-I).

However, few TUNEL-positive bodies are observed at the equivalent stage and location in the mouse (Laemle et al. 1999; Trousse et al. 2001). It is accepted that this area plays a role in the morphogenesis of the optic cup. (ii) Concerning to the optic pathways, a large number of cells die in the presumptive optic chiasm during optic cup stages (St21–23), and (iii) abundant dead neuroepithelial cells are found along the distal half of the optic stalk between St27 and St29. These areas of cell death in the optic pathways are concomitant with the ganglion cell differentiation in the chick (Silver et al. 1987; Navascués et al. 1988; Charvet & Striedter, 2008), mouse (Rodríguez-Gallardo et al. 2005) and rat (Horsburgh & Sefton, 1986). Differentiating ganglion cells can be identified immunohistochemically in the small-spotted catshark between St26 and St28 (Ferreiro-Galve et al. 2008; Bejarano-Escobar et al. 2012a). Therefore, degenerating neuroepithelial cells detected in the distal half of the optic stalk by these stages could provide a pathway of minimal resistance for the incoming ganglion cell axons. However, cell death detected in the *S. canicula* presumptive optic chiasm occurs much earlier in development, during invagination of the optic vesicle to form the optic cup (St21–23). The location of dying cells in the chiasmatic region by these early stages could be correlated with the ongoing morphogenesis of the central nervous system. Some authors claim that this region of cell degeneration might be responsible for the ventral shifting of the optic stalk (Källén, 1955; Knabe et al. 2000). (iv) Finally, between St23 and St26, an area of cell death is apparent in the anterior wall of the developing lens during detachment of the lens anlage from the cephalic ectoderm, as has been described in other vertebrates (Silver & Hughes, 1973; Cuadros et al. 1991; Lang, 1997; Knabe & Kuhn, 1998; Laemle et al. 1999; Nishitani & Sasaki, 2006).

From St18 to St29, scattered dying cells can also be found dispersed throughout the neuroepithelium of the

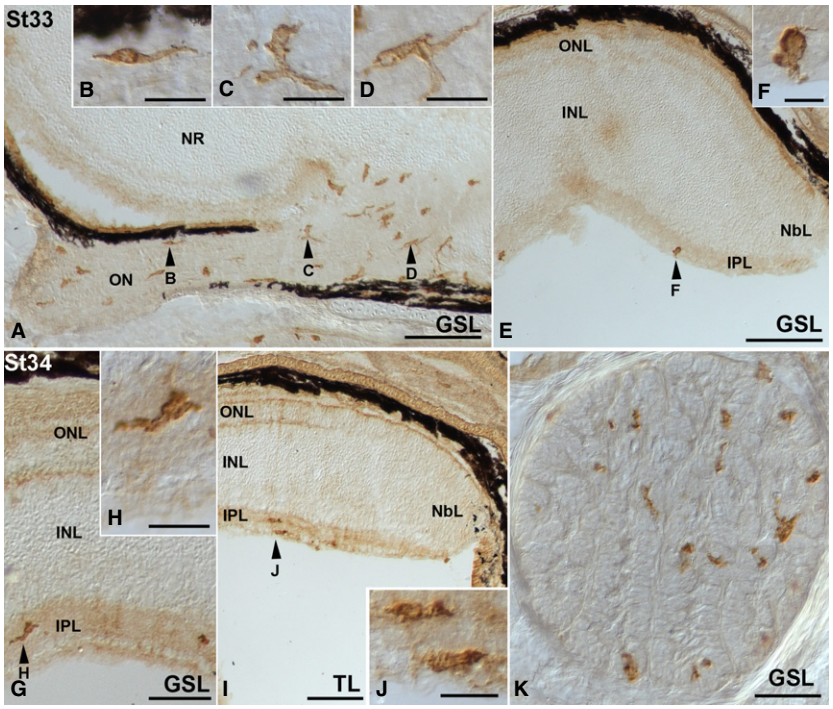


**Fig. 8** Lectin-positive cells in the developing visual system of small-spotted catshark embryos during St33 (A-F) and St34 (G-K). Frontal (A-J) and sagittal (K) cryosections of the head were treated according to the GSL (A-H,K) and TL (I,J) histochemistry technique. Arrowheads in (A,E,G) and (I) point to cells shown at higher magnification in (B-D,F,H) and (J). In all panels, dorsal is up. Lectin-positive amoeboid cells with short processes and distinct morphologies (B-D) were visible in the optic nerve (A). Sparse round labelled cells were observed in the vitreal-most region of the peripheral retina (E,F). At St34, lectin-positive cells colonized the IPL of the central (G,H) and peripheral (I,J) retina. A section transverse to the optic nerve showed that labelled cells were homogeneously distributed (K). GSL, *Griffonia simplicifolia* lectin; INL, inner nuclear layer; IPL, inner plexiform layer; NbL, neuroblastic layer; NR, neural retina; ON, optic nerve; ONL, outer nuclear layer; TL, tomato lectin. Scale bars: 200 μm (A,E); 20 μm (B-D,H,J); 100 μm (G); 50 μm (K); 10 μm (F).

undifferentiated retina, as has previously been described in several vertebrates (Young, 1984; Cuadros & Ríos, 1988; Martín-Partido et al. 1988; Cook et al. 1998; Diaz et al. 1999; Laemle et al. 1999; Pequignot et al. 2003; Bejarano-Escobar et al. 2011) including fish (Candal et al. 2005; Bejarano-Escobar et al. 2010). By these stages, degenerating cells have been characterized as proliferating cells (Diaz et al. 1999; Candal et al. 2005; Valenciano et al. 2009).

*Cell death during retinal histogenesis*

The incidence of cell death in the *S. canicula* developing retina during stages where the emergence of the retinal layers takes place (St30 onwards), and the perinatal and adult ages is discussed in this section. Recently we have reported that the maturation of the retinal layers and the appearance of neurochemical profiles in the small-spotted catshark follow a central-to-peripheral gradient (Bejarano-Escobar et al. 2012a), as in the rest of vertebrates (Sharma & Ungar, 1980; Young, 1984; Prada et al. 1991; Hu & Easter, 1999; Candal et al. 2005, 2008; Francisco-Morcillo et al. 2006; Kitambi & Malicki, 2008; Bejarano-Escobar et al. 2009, 2010). Furthermore, histogenesis and cell differentiation also progress in a vitreal-to-scleral manner (Bejarano-Escobar et al. 2012a). Here we found that the sequence of histogenetic cell death in the *S. canicula* retina apparently recapitulates the sequence of maturation of the various layers and cell types, starting in the GCL and proceeding to more external layers, as has been described in other vertebrates (Young, 1984; Beazley et al. 1987; Cook et al. 1998; Marín-Teva et al. 1999). During shark retinal differentiation, degenerating cells were found in all nuclear layers (GCL, INL and ONL), as has been observed in other fish species (Hoke & Fernald, 1998; Biehlmaier et al. 2001; Cole & Ross, 2001; Candal et al. 2005; Bejarano-Escobar et al. 2010), turtle (Francisco-Morcillo et al. 2004), mouse (Young, 1984; Bejarano-Escobar et al. 2011) and rat (Beazley et al. 1987). However, no dying cells were seen in the ONL in the chick or quail (Cook et al. 1998; Marín-Teva et al. 1999).

*Ontogenetic cell death in the visual system of fish*

To date, there is still a paucity of information on developmental cell death in the visual system of teleost species (Hoke & Fernald, 1998; Biehlmaier et al. 2001; Cole & Ross, 2001; Candal et al. 2005; Iijima & Yokoyama, 2007; Bejarano-Escobar et al. 2010) and, to the best of our knowledge, previous to the present study, there were no

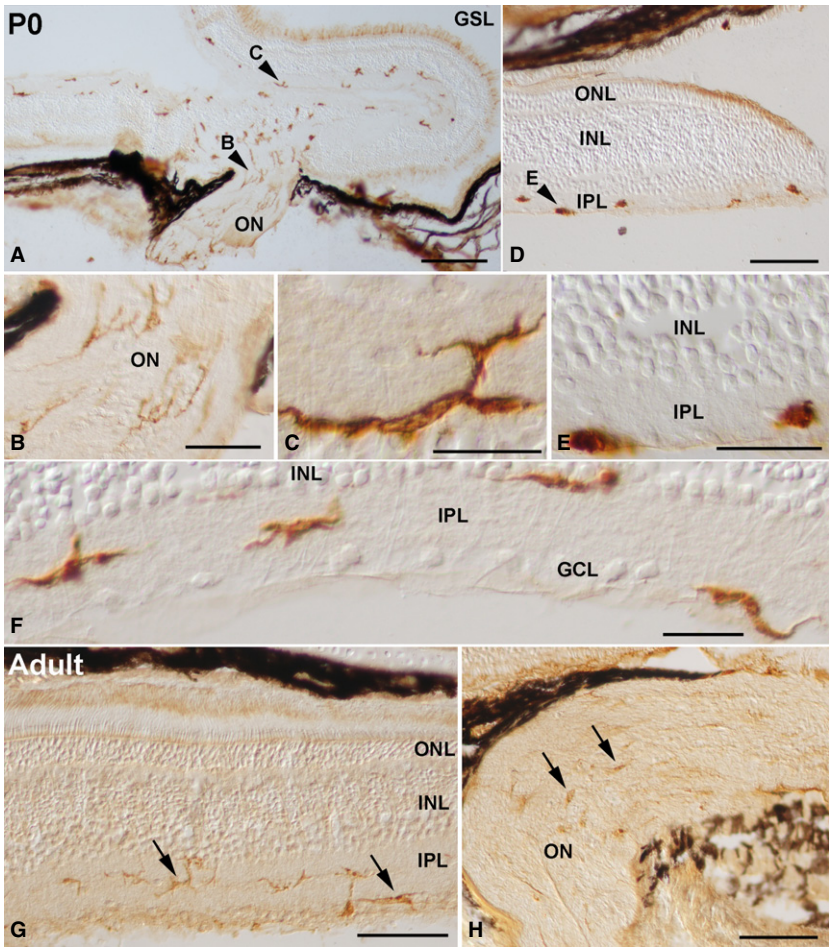


**Fig. 9** Spatial pattern of lectin-positive cells in the P0 (A-F) and adult (G,H) retina of the small-spotted catshark. Cryosections from retinas were treated according to the GSL histochemistry technique. Arrowheads in (A,D) point to cells shown at higher magnification in (B,C,E). Abundant ramified lectin-positive cells that extended thin processes coursing parallel to the ganglion cell axons were detectable in the optic nerve (A,B). Many ramified labelled cells were also distinguishable in the IPL of the central retina (A,C,F). Lectin-positive cells in the peripheral regions of the retina were round and amoeboid in shape (D,E). At P0, most of the labelled cells were oriented parallel to the vitreal surface, and showed a stratification pattern within the IPL: they were located in the border between the IPL and the INL, in the border between the IPL and the GCL, and in the middle of the IPL (F). In the adult shark visual system, the intensity of lectin labelling diminished (arrows in G,H). Lectin-positive cells showed a well ramified shape, with most of their processes oriented parallel to the vitreal surface of the retina (arrows in G). Note that labelled cells were mainly located in the IPL (arrows in G). Lectin-positive cells in the optic nerve revealed a weak histochemical signal (arrows in H). GCL, ganglion cell layer; GSL, *Griffonia simplicifolia* lectin; INL, inner nuclear layer; IPL, inner plexiform layer; ON, optic nerve; ONL, outer nuclear layer. Scale bars: 200 μm (A,D); 50 μm (B); 20 μm (C,E,F); 100 μm (G,H).

data available on ontogenetic cell death in elasmobranch species. Our results differ from those reported in most of the teleost species, because those studies found that cell death was restricted to sparse cells, generally well separated, with no clear concentration or pattern (Hoke & Fernald, 1998; Cole & Ross, 2001; Bejarano-Escobar et al. 2010). However, Candal et al. (2005) were able to distinguish different waves of cell death in the brown trout retina, coinciding with the formation of the optic cup, with retinal histogenesis and with photoreceptor differentiation, respectively. The differences in the spatiotemporal patterns of cell death during retinal ontogenesis among fish could be related to differences in the time course of retinal growth, as brown trout and *S. canicula* have a very protracted embryonic development, whereas most other teleost models have a rapid development to maturity. In particular, during development of the *S. canicula* visual system, the main areas of cell death reported in the literature for the other vertebrate species that have been studied are observed. However, it is important to note that we were not able to detect the sub-optic necrotic centres (SONCs) during development of the shark visual system. SONCs are located at the diencephalic insertion of the optic stalks, and are considered the most strictly localized and intense foci of degeneration in the early developing brain in mammals and birds

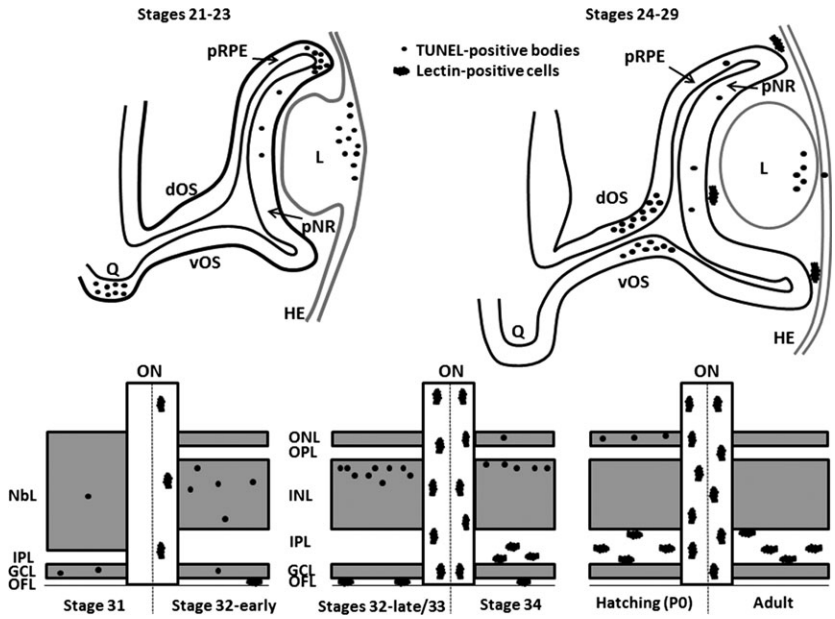


**Fig. 10** Schematic drawings showing the spatiotemporal distribution of TUNEL-positive bodies and lectin-positive cells in the developing visual system of the small-spotted catshark. During early stages, TUNEL-positive bodies are found to be accumulated in four precise and spatiotemporally distinct locations: the presumptive optic chiasm (St21–23), the dorsal-most part of the optic cup (St21–23), the lens tissue (St23–26) and the distal optic stalk (St27–29). During these early stages, TUNEL-positive bodies are sparse in the undifferentiated neural retina. However, during the period of retinal histogenesis and cell differentiation (St31 onwards), a clear vitreal-to-scleral gradient of cell death occurs, affecting cells located in the three nuclear layers. By the early stages of development (St24–31), lectin-positive cells are absent from the nervous parenchyma and are only present in the vitreous cavity of the optic anlage. From St32-early onwards, many lectin-positive cells are detectable along the entire length of the optic nerve. Furthermore, lectin-positive cells are seen to colonize progressively more scleral retinal layers as development advances, to gain access to the IPL. dOS, dorsal optic stalk; GCL, ganglion cell layer; HE, head ectoderm; INL, inner nuclear layer; IPL, inner plexiform layer; L, lens; NbL, neuroblastic layer; OFL, optic fiber layer; ON, optic nerve; ONL, outer nuclear layer; OPL, outer plexiform layer; pNR, presumptive neural retina; pRPE, presumptive retinal pigment epithelium; Q, optic chiasm; vOS, ventral optic stalk.

(Silver et al. 1987; Navascués et al. 1988; Martín-Partido et al. 1991; Knabe & Kuhn, 1998). Overall, our findings support the view that, during visual system development, there are differences in the topographic pattern of cell death in vertebrates.

## Lectin-positive cells in the developing *S. canicula* visual system

The morphological features and topographical distribution patterns of GSL-/TL-positive cells allow them to be characterized as macrophages and microglial cells. Moreover, lectin-positive cells in the *S. canicula* developing visual system apparently pass through different morphological stages of development, highly coincident with those described during the transformation of amoeboid microglia into ramified microglia (Cuadros & Navascués, 1998). Therefore, the present investigation demonstrates the usefulness of lectin-histochemical techniques in the study of the development of specialized phagocytes in the developing *S. canicula* visual system. However, due to the lack of a specific marker for macrophages/microglia in this species, we cannot confirm that all forms of macrophages/microglial cells could be detected with lectin histochemistry.

### *Chronotopographical distribution and morphological features of lectin-positive cells*

No lectin-positive phagocytes were detected in either the developing retina or the visual pathways of the shark before St32-early. Only some lectin-positive cells appeared in the vitreous from St29 to St31, as has been described previously in the developing visual system of other vertebrates (Ashwell, 1989; Cuadros et al. 1991; Navascués et al. 1995; Nishitani & Sasaki, 2006; Santos et al. 2008; Bejarano-Escobar et al. 2011). Specialized lectin-positive phagocytes were first detected homogeneously distributed in the St32-early *S. canicula* optic nerve. Only a few studies have dealt with the ontogeny of specialized phagocytes during development of the vertebrate optic pathways (Martín-Partido & Navascués, 1990; Martín-Partido et al. 1991; Moujahid et al. 1996; Rodríguez-Gallardo et al. 2005; Bejarano-Escobar et al. 2011). Macrophages have been observed in the optic stalk in intimate contact with the first optic fibre bundles in rodents (Rodríguez-Gallardo et al. 2005) and birds (Moujahid et al. 1996), suggesting a possible involvement of these cells in optic axon growth. In *S. canicula* the first ganglion cells differentiate at St26 (see above), and by St32-early the optic nerve is apparently occupied by abundant optic axonal fascicles. Therefore, these lectin-positive cells

do not seem to participate in either growth of pioneering optic axons or the guidance of the following axons in the shark developing optic pathways.

Concerning the retinal distribution of lectin-positive phagocytes during development of the *S. canicula* visual system, sparse labelled cells were first detected at St32-early. They were located in the OFL, close to the optic nerve head. As development progressed, the area occupied by microglial precursors spread along a central-to-peripheral gradient. These amoeboid phagocytes apparently migrated parallel to the optic fascicles of the OFL, as has been shown in the avian retina (Navascués et al. 1995) and then reached other retinal layers by radial migration, as has been described in the mammalian (Santos et al. 2008; Bejarano-Escobar et al. 2011) and avian retinas (Navascués et al. 1995; Cuadros & Navascués, 1998). This central-to-peripheral and vitreal-to-scleral migration of microglial precursors in the developing *S. canicula* retina was corroborated by observations in P0 retinas, showing that, while labelled cells in peripheral regions of the retina were amoeboid in shape, abundant ramified lectin-positive cells were located exclusively in central regions. Our observations support the entry of an appreciable number of new microglial cells into the retina from the optic nerve head, as has been reported in other vertebrates (Navascués et al. 1995; Provis et al. 1996) but we cannot rule out the entry of some microglial cells from other regions, such as the vitreous body.

In the adult *S. canicula* retina, lectin-positive cells were mainly confined to the IPL and GCL, as has been described in the rabbit retina (Ashwell, 1989; Schnitzer, 1989). However, microglial cells can be distinguished in the OFL, GCL, IPL and OPL, and occasionally in the INL, in the retina of other mammals (Boycott & Hopkins, 1981; Díaz-Araya et al. 1995; Santos et al. 2008; Bejarano-Escobar et al. 2011) and birds (Navascués et al. 1995).

### Correlation between the chronotopographical pattern of the distribution of cell death and lectin-positive phagocytes

No chronotopographical relationship was found between lectin-positive phagocytes and TUNEL-positive bodies in the developing *S. canicula* visual system. Thus, in the early stages, whereas extensive areas of cell death were observed in the dorsal rim of the optic cup, lens anlage, distal optic stalk and presumptive optic chiasm, no lectin-positive cells were detected in topographical coincidence with TUNEL-positive bodies. Furthermore, in the differentiating retina, cell death and lectin-positive cells were not seen simultaneously in the same retinal layers. Therefore, cell death is not the attracting stimulus for macrophage/microglial cells migrating into the developing visual system, as has been proposed in other vertebrate species (Hume et al. 1983; Schnitzer, 1989; Moujahid et al. 1996; Rodríguez-Gallardo et al. 2005; Santos et al. 2008; Bejarano-Escobar et al. 2011). Thus, in most species, this hypothesis is sustained by the chronological coincidence of cell death with the entry of microglia into the nervous parenchyma (Hume et al. 1983; Schnitzer, 1989; Ashwell, 1990; Perry & Gordon, 1991; Knabe et al. 2000; Rodríguez-Gallardo et al. 2005; Santos et al. 2008; Bejarano-Escobar et al. 2011), and by the phagocytosis of neuronal debris by macrophages and microglial cells in areas of cell degeneration (Ashwell, 1990; Martín-Partido & Navascués, 1990; Egensperger et al. 1996; Moujahid et al. 1996; Thanos et al. 1996; Rodríguez-Gallardo et al. 2005). Therefore, other cells within the *S. canicula* visual system have to be involved in the clearance of cell debris during development. Thus, phagocytic activity of neuroepithelial and Müller cells has been reported previously during normal vertebrate retinal development (Navascués et al. 1988; Martín-Partido & Navascués, 1990; Egensperger et al. 1996; Marín-Teva et al. 1999; Bejarano-Escobar et al. 2011) and in the injured fish retina (Bailey et al. 2010; Bejarano-Escobar et al. 2012b). The characterization of non-specialized phagocytes that participate in the removal of apoptotic cell debris during ontogenetic cell death in the *S. canicula* visual system cannot be ignored and merits further investigation.

### Concluding remarks

Elasmobranchs occupy a key phylogenetic position as an out-group to osteichthyans, and therefore knowledge of different aspects of their retinal ontogeny is essential to assess the ancestral condition in gnathostomes and evolution of visual system development in vertebrates. The present study shows that ontogenetic cell death in the developing visual system of *S. canicula* occurs with similar but not identical spatiotemporal-restricted patterns to that observed in other vertebrates. This study also shows that the spatiotemporal patterns of lectin-positive phagocytes are not coincident with that of cell death.

## Acknowledgements

We are grateful to Eva Candal, University of Santiago de Compostela, La Coruña, Spain, for critical reading of the manuscript. We express our gratitude to María Salud Holguín Arévalo for her excellent technical assistance and Manuel Ramírez for assistance with microscopy. Special thanks are also due to the skippers of the fishing vessels *Torrejaral* and *Rafael y Antonio*. R.B.E. is a recipient of a PhD studentship from the *Junta de Extremadura*. This work was supported by Grants from the Spanish Ministerio de Ciencia y Tecnología (BFU2007-67540) and Junta de Extremadura (PRI06A195).

## References

**Acarín L, Vela JM, González B, et al.** (1994) Demonstration of poly-N-acetyl lactosamine residues in ameboid and ramified microglial cells in rat brain by tomato lectin binding. *J Histochem Cytochem* **42**, 1033–1041.

**Ashwell K** (1989) Development of microglia in the albino rabbit retina. *J Comp Neurol* **287**, 286–301.

**Ashwell K** (1990) Microglia and cell death in the developing mouse cerebellum. *Brain Res Dev Brain Res* **55**, 219–230.

**Bailey TJ, Fossum SL, Fimbel SM, et al.** (2010) The inhibitor of phagocytosis, O-phospho-L-serine, suppresses Müller glia proliferation and cone cell regeneration in the light-damaged zebrafish retina. *Exp Eye Res* **91**, 601–612.

**Ballard WW, Mellinger J, Lechenault H** (1993) A Series of Normal Stages for Development of *Scyliorhinus Canicula*, the Lesser Spotted Dogfish (Chondrichthyes: Scyliorhinidae). *J Exp Zool* **267**, 318–336.

**Beazley LD, Perry VH, Baker B, et al.** (1987) An investigation into the role of ganglion cells in the regulation of division and death of other retinal cells. *Brain Res* **430**, 169–184.

**Bejarano-Escobar R, Blasco M, DeGrip WJ, et al.** (2009) Cell differentiation in the retina of an epibenthonic teleost, the Tench (Tinca tinca, Linneo 1758). *Exp Eye Res* **89**, 398–415.

**Bejarano-Escobar R, Blasco M, Degrip WJ, et al.** (2010) Eye development and retinal differentiation in an altricial fish species, the Senegalese sole (*Solea senegalensis*, Kaup 1858). *J Exp Zool B Mol Dev Evol* **314**, 580–605.

**Bejarano-Escobar R, Holguín-Arevalo MS, Montero JA, et al.** (2011) Macrophage and microglia ontogeny in the mouse visual system can be traced by the expression of Cathepsins B and D. *Dev Dyn* **240**, 1841–1855.

**Bejarano-Escobar R, Blasco M, Durán AC, et al.** (2012a) Retinal histogenesis and cell differentiation in an elasmobranch species, the small-spotted catshark *Scyliorhinus canicula*. *J Anat* **220**, 318–335.

**Bejarano-Escobar R, Blasco M, Martín-Partido G, et al.** (2012b) Light-induced degeneration and microglial response in the retina of an epibenthonic pigmented teleost: age-dependent photoreceptor susceptibility to cell death. *J Exp Biol* **215**, 3799–3812.

**Biehlmaier O, Neuhauss SC, Kohler K** (2001) Onset and time course of apoptosis in the developing zebrafish retina. *Cell Tissue Res* **306**, 199–207.

**Boycott BB, Hopkins JM** (1981) Microglia in the retina of monkey and other mammals: its distinction from other types of glia and horizontal cells. *Neuroscience* **6**, 679–688.

**Candal E, Anadón R, DeGrip WJ, et al.** (2005) Patterns of cell proliferation and cell death in the developing retina and optic tectum of the brown trout. *Brain Res Dev Brain Res* **154**, 101–119.

**Candal E, Ferreiro-Galve S, Anadón R, et al.** (2008) Morphogenesis in the retina of a slow-developing teleost: emergence of the GABAergic system in relation to cell proliferation and differentiation. *Brain Res* **1194**, 21–27.

**Charvet CJ, Striedter GF** (2008) Spatiotemporal clustering of cell death in the avian forebrain proliferative zone. *Int J Dev Biol* **52**, 345–352.

**Cole LK, Ross LS** (2001) Apoptosis in the developing zebrafish embryo. *Dev Biol* **240**, 123–142.

**Cook B, Portera-Cailliau C, Adler R** (1998) Developmental neuronal death is not a universal phenomenon among cell types in the chick embryo retina. *J Comp Neurol* **396**, 12–19.

**Cuadros MA, Navascués J** (1998) The origin and differentiation of microglial cells during development. *Prog Neurobiol* **56**, 173–189.

**Cuadros MA, Ríos A** (1988) Spatial and temporal correlation between early nerve fiber growth and neuroepithelial cell death in the chick embryo retina. *Anat Embryol (Berl)* **178**, 543–551.

**Cuadros MA, Martin C, Ríos A, et al.** (1991) Macrophages of hemanglioblastic lineage invade the lens vesicle ectoderm interspace during closure and detachment of the avian embryionic lens. *Cell Tissue Res* **266**, 117–127.

**Diaz B, Pimentel B, de Pablo F, et al.** (1999) Apoptotic cell death of proliferating neuroepithelial cells in the embryonic retina is prevented by insulin. *Eur J Neurosci* **11**, 1624–1632.

**Díaz-Araya CM, Provis JM, Penfold PL, et al.** (1995) Development of microglial topography in human retina. *J Comp Neurol* **363**, 53–68.

**Egensperger R, Maslim J, Bisti S, et al.** (1996) Fate of DNA from retinal cells dying during development: uptake by microglia and macroglia (Müller cells). *Brain Res Dev Brain Res* **97**, 1–8.

**Ferreiro-Galve S, Candal E, Carrera I, et al.** (2008) Early development of GABAergic cells of the retina in sharks: an immunohistochemical study with GABA and GAD antibodies. *J Chem Neuroanat* **36**, 6–16.

**Ferreiro-Galve S, Rodríguez-Moldes I, Anadón R, et al.** (2010a) Patterns of cell proliferation and rod photoreceptor differentiation in shark retinas. *J Chem Neuroanat* **39**, 1–14.

**Ferreiro-Galve S, Rodríguez-Moldes I, Candal E** (2010b) Calretinin immunoreactivity in the developing retina of sharks: comparison with cell proliferation and GABAergic system markers. *Exp Eye Res* **91**, 378–386.

**Ferreiro-Galve S, Rodríguez-Moldes I, Candal E** (2012) Pax6 expression during retinogenesis in sharks: comparison with markers of cell proliferation and neuronal differentiation. *J Exp Zool B Mol Dev Evol* **318**, 91–108.

**Francisco-Morcillo J, Hidalgo-Sánchez M, Martín-Partido G** (2004) Spatial and temporal patterns of apoptosis during differentiation of the retina in the turtle. *Anat Embryol (Berl)* **208**, 289–299.

**Francisco-Morcillo J, Hidalgo-Sánchez M, Martín-Partido G** (2006) Spatial and temporal patterns of proliferation and differentiation in the developing turtle eye. *Brain Res* **1103**, 32–48.

**García-Porrero JA, Colvee E, Ojeda JL** (1984) Cell death in the dorsal part of the chick optic cup. Evidence for a new necrotic area. *J Embryol Exp Morphol* **80**, 241–249.

**Herbomel P, Thisse B, Thisse C** (2001) Zebrafish early macrophages colonize cephalic mesenchyme and developing brain, retina, and epidermis through a M-CSF receptor-dependent invasive process. *Dev Biol* **238**, 274–288.

**Hidalgo-Sánchez M, Francisco-Morcillo J, Navascués J, et al.** (2007) Early development of the optic nerve in the turtle *Mauremys leprosa*. *Brain Res* **1137**, 35–49.

**Hoke KL, Fernald RD** (1998) Cell death precedes rod neurogenesis in embryonic teleost retinal development. *Brain Res Dev Brain Res* **111**, 143–146.

**Horsburgh GM, Sefton AJ** (1986) The early developmental of optic nerve and chiasm in embryonic rat. *J Comp Neurol* **243**, 547–560.

**Hu M, Easter SS** (1999) Retinal neurogenesis: the formation of the initial central patch of postmitotic cells. *Dev Biol* **207**, 309–321.

**Hume DA, Perry VH, Gordon S** (1983) Immunohistochemical localization of a macrophage-specific antigen in developing mouse retina: phagocytosis of dying neurons and differentiation of microglial cells to form a regular array in the plexiform layers. *J Cell Biol* **97**, 253–257.

**Iijima N, Yokoyama T** (2007) Apoptosis in the medaka embryo in the early developmental stage. *Acta Histochem Cytochem* **40**, 1–7.

**Jimeno D, Velasco A, Lillo C, et al.** (1999) Response of microglial cells after a cryolesion in the peripheral proliferative retina of tench. *Brain Res* **816**, 175–189.

**Jimeno D, Lillo C, Cid E, et al.** (2003) The degenerative and regenerative processes after the elimination of the proliferative peripheral retina of fish. *Exp Neurol* **179**, 210–228.

**Källén B** (1955) Cell degeneration during normal ontogenesis of the rabbit brain. *J Anat* **89**, 153–161.

**Kaur C, Ling EA** (1991) Study of the transformation of amoeboid microglial cells into microglia labelled with the isolectin *Griffonia simplicifolia* in postnatal rats. *Acta Anat (Basel)* **142**, 118–125.

**Kitambi SS, Malicki JJ** (2008) Spatiotemporal features of neurogenesis in the retina of medaka, *Oryzias latipes*. *Dev Dyn* **237**, 3870–3881.

**Knabe W, Kuhn HJ** (1998) Pattern of cell death during optic cup formation in the tree shrew *Tupaia belangeri*. *J Comp Neurol* **401**, 352–366.

**Knabe W, Suss M, Kuhn HJ** (2000) The patterns of cell death and of macrophages in the developing forebrain of the tree shrew *Tupaia belangeri*. *Anat Embryol (Berl)* **201**, 157–168.

**Laemle LK, Puszkarczuk M, Feinberg RN** (1999) Apoptosis in early ocular morphogenesis in the mouse. *Dev Brain Res* **112**, 129–133.

**Lang RA** (1997) Apoptosis in mammalian eye development: lens morphogenesis, vascular regression and immune privilege. *Cell Death Differ* **4**, 12–20.

**Marín-Teva JL, Cuadros MA, Calvente R, et al.** (1999) Naturally occurring cell death and migration of microglial precursors in the quail retina during normal development. *J Comp Neurol* **412**, 255–275.

**Martín-Partido G, Navascués J** (1990) Macrophage-like cells in the presumptive optic pathways in the floor of the diencephalon of the chick embryo. *J Neurocytol* **19**, 820–832.

**Martín-Partido G, Rodríguez-Gallardo L, Álvarez IS, et al.** (1988) Cell death in the ventral region of the neural retina during the early development of the chick embryo eye. *Anat Rec* **222**, 272–281.

**Martín-Partido G, Cuadros MA, Martin C, et al.** (1991) Macrophage-like cells invading the suboptic necrotic centres of the avian embryo diencephalon originate from haemopoietic precursors. *J Neurocytol* **20**, 962–968.

**Mayordomo R, Valenciano AI, de la Rosa EJ, et al.** (2003) Generation of retinal ganglion cells is modulated by caspase-dependent programmed cell death. *Eur J Neurosci* **18**, 1744–1750.

**Moujahid A, Navascués J, Marín-Teva JL, et al.** (1996) Macrophages during avian optic nerve development: relationship to cell death and differentiation into microglia. *Anat Embryol* **193**, 131–144.

**Nagata S** (2005) DNA degradation in development and programmed cell death. *Annu Rev Immunol* **23**, 853–875.

**Navascués J, Martín-Partido G, Álvarez IS, et al.** (1988) Cell death in suboptic necrotic centers of chick embryo diencephalon and their topographic relationship with the earliest optic fiber fascicles. *J Comp Neurol* **278**, 34–46.

**Navascués J, Moujahid A, Almendros A, et al.** (1995) Origin of microglia in the quail retina: central-to-peripheral and vitreal-to-scleral migration of microglial precursors during development. *J Comp Neurol* **354**, 209–228.

**Nishitani K, Sasaki K** (2006) Macrophage localization in the developing lens primordium of the mouse embryo – an immunohistochemical study. *Exp Eye Res* **83**, 223–228.

**Oppenheim RW** (1991) Cell death during development of the nervous system. *Annu Rev Neurosci* **14**, 453–501.

**Pequignot MO, Provost AC, Salle S, et al.** (2003) Major role of BAX in apoptosis during retinal development and in establishment of a functional postnatal retina. *Dev Dyn* **228**, 231–238.

**Perry VH, Gordon S** (1991) Macrophages and the nervous system. *Int Rev Cytol* **125**, 203–244.

**Prada C, Puga J, Pérez-Méndez L, et al.** (1991) Spatial and temporal patterns of neurogenesis in the chick retina. *Eur J Neurosci* **3**, 559–569.

**Provis JM, Díaz CM, Penfold PL** (1996) Microglia in human retina: a heterogeneous population with distinct ontogenies. *Perspect Dev Neurobiol* **3**, 213–222.

**Rodríguez-Gallardo L, Lineros-Domínguez MC, Francisco-Morcillo J, et al.** (2005) Macrophages during retina and optic nerve development in the mouse embryo: relationship to cell death and optic fibres. *Anat Embryol (Berl)* **210**, 303–316.

**Santos AM, Calvente R, Tassi M, et al.** (2008) Embryonic and postnatal development of microglial cells in the mouse retina. *J Comp Neurol* **506**, 224–239.

**Schnitzer J** (1989) Enzyme-histochemical demonstration of microglial cells in the adult and postnatal rabbit retina. *J Comp Neurol* **282**, 249–263.

**Sharma SC, Ungar F** (1980) Histogenesis of the goldfish retina. *J Comp Neurol* **191**, 373–382.

**Silver J, Hughes FW** (1973) The role of cell death during morphogenesis of the mammalian eye. *J Morphol* **140**, 159–170.

**Silver J, Poston M, Rutishauser U** (1987) Axon pathway boundaries in the developing brain. I. Cellular and molecular determinants that separate the optic and olfactory projections. *J Neurosci* **7**, 2264–2272.

**Streit A, Faissner A, Gehrig B, et al.** (1990) Isolation and biochemical characterization of a neural proteoglycan expressing the L5 carbohydrate epitope. *J Neurochem* **55**, 1494–1506.

**Thanos S, Moore S, Hong YM** (1996) Retinal microglia. *Prog Retin Eye Res* **15**, 331–361.

**Trousse F, Esteve P, Bovolenta P** (2001) Bmp4 mediates apoptotic cell death in the developing chick eye. *J Neurosci* **21**, 1292–1301.

**Valenciano AI, Boya P, de la Rosa EJ** (2009) Early neural cell death: numbers and cues from the developing neuroretina. *Int J Dev Biol* **53**, 1515–1528.

**Velasco A, Caminos E, Vecino E, et al.** (1995) Microglia in normal and regenerating visual pathways of the tench (*Tinca tinca* L., 1758; Teleost): a study with tomato lectin. *Brain Res* **705**, 315–324.

**Yeo W, Gautier J** (2003) A role for programmed cell death during early neurogenesis in *Xenopus*. *Dev Biol* **260**, 31–45.

**Young RW** (1984) Cell death during differentiation of the retina in the mouse. *J Comp Neurol* **229**, 362–373.